Structural Engineering and Mechanics, *Vol. 74, No. 2 (2020) 175-187*
DOI: https://doi.org/10.12989/sem.2020.74.2.175

Buckling and free vibration analyses of nanobeams with surface effects via various higher-order shear deformation theories

Omid Rahmani*[1] and S. Samane Asemani[2a]

[1]*Structures and New Advanced Materials Laboratory Department of Mechanical Engineering, University of Zanjan, Zanjan, Iran*
[2]*Department of Mechanical Engineering, University of Tarbiat Modares, Tehran, Iran*

(Received October 2, 2017, Revised December 26, 2017, Accepted December 14, 2019)

Abstract. The theories having been developed thus far account for higher-order variation of transverse shear strain through the depth of the beam and satisfy the stress-free boundary conditions on the top and bottom surfaces of the beam. A shear correction factor, therefore, is not required. In this paper, the effect of surface on the axial buckling and free vibration of nanobeams is studied using various refined higher-order shear deformation beam theories. Furthermore, these theories have strong similarities with Euler–Bernoulli beam theory in aspects such as equations of motion, boundary conditions, and expressions of the resultant stress. The equations of motion and boundary conditions were derived from Hamilton's principle. The resultant system of ordinary differential equations was solved analytically. The effects of the nanobeam length-to-thickness ratio, thickness, and modes on the buckling and free vibration of the nanobeams were also investigated. Finally, it was found that the buckling and free vibration behavior of a nanobeam is size-dependent and that surface effects and surface energy produce significant effects by increasing the ratio of surface area to bulk at nano-scale. The results indicated that surface effects influence the buckling and free vibration performance of nanobeams and that increasing the length-to-thickness increases the buckling and free vibration in various higher-order shear deformation beam theories. This study can assist in measuring the mechanical properties of nanobeams accurately and designing nanobeam-based devices and systems.

Keywords: higher-order shear; surface effect; elastic medium; axial bulking; analytical modeling

1. Introduction

It is well known that the elementary theory of bending the beam based on Euler-Bernoulli hypothesis disregards the effects of shear deformation and stress concentration. This theory is suitable for slender beams rather than thick or deep beams since it is based on the assumption that the sections normal to neutral axis before bending remain so during bending and after bending, implying that the transverse shear strain is zero. Since this theory neglects the transverse shear deformation, it underestimates deflections in the case of thick beams where the effects of shear deformation are significant. The discrepancies in the elementary theory of beam bending and first-order shear deformation theory require the improvement of higher-order or equivalent refined shear deformation theories. Euler-Bernoulli elementary theory of bending (ETB) of beam (2011) disregards the effect of shear deformation. The first-order shear deformation theory (FSDT) of Timoshenko (1921) includes refined effects such as the rotatory inertia and shear deformation in the beam theory. Cowper (1966) gave a refined expression for the shear correction factor for different cross-sections of the beam. Levinson (1981), Bickford (1982), Rehfield and Murthy (1982), Krishna Murty (1984), Baluch *et al.* (1984), and Bhimaraddi and Chandrashekhara (1993) presented parabolic shear deformation theories, assuming a higher variation of axial displacement in terms of thickness coordinate. Kant and Gupta (1988) and Heyliger and Reddy (1988) presented higher-order shear deformation theories for the static and free vibration analyses of shear-deformable uniform rectangular beams. There is an alternative class of refined theories, which consists of trigonometric functions to characterize the shear deformation effects through the thickness of the beam. Vlasov and Leont'ev (1966) and Stein (1989) developed refined shear deformation theories for thick beams, including sinusoidal function in terms of thickness coordinate in the displacement field. However, by applying these theories, shear stress-free boundary conditions are not satisfied on the top and bottom surfaces of the beam. Abdelaziz *et al.* (2017) developed a hyperbolic shear deformation theory and applied for the bending, vibration and buckling of PGM sandwich plate with various boundary conditions. Meziane *et al.* (2014) presented a shear deformation theory for the vibration and buckling of exponentially graded material sandwich plate resting on elastic foundations under various boundary conditions. The displacement field of the present theory was chosen based on nonlinear variations in the in-plane displacements through the thickness of the plate. Ghugal and Sharma (2009) developed the variationally consistent, hyperbolic shear deformation theory for flexural analysis of thick beams and obtained the displacements, stresses, and fundamental frequencies of flexural mode and thickness shear modes from free vibration of simply supported beams.

*Corresponding author, Ph.D.
E-mail: omid.rahmani@znu.ac.ir
[a] Ph.D. Student

ISSN: 1225-4568 (Print), 1598-6217 (Online)

Challamel and Wang (2011) studied the lateral-torsional buckling problem of Eringen's study based on the static and dynamic deformation of thick, functionally graded, elastic plates by using higher-order shear and normal deformable plate theories and meshless local Petrov–Galerkin method. Rao and Ganesan (1995) investigated the harmonic response of tapered composite beams by employing finite element model based on a higher-order shear deformation theory. Khdeir and Reddy (1997) presented an exact solution to the governing equations for bending the laminated beams. They employed the classical, the first-order, the second-order, and the third-order beam theories in their analysis. They studied the effect of shear deformation, the number of layers, and the orthotropic ratio on the static response of composite beams. They found big differences between the deflections predicted by the classical beam theory and those predicted by the higher-order beam theories, especially when the ratio of beam length to its height was low due to the shear deformation effects. Eisenberger (2003) proposed exact stiffness coefficients, including the cubic variations of the axial displacements over the cross-section of the beam, for isotropic beam by employing a simple higher-order theory. Subramanian (2006) proposed the free vibration analysis of composite beams using finite elements based on two higher-order shear deformation theories. Wang *et al*. (2010) studied these small-scale structures and presented some scale effects that can be captured using nonlocal mechanics. Bouafia *et al*. (2017) investigated size dependent bending and free flexural vibration behaviors of FG nanobeams using a nonlocal quasi-3D theory in which both shear deformation and thickness stretching effects were introduced. Zemri *et al*. (2015) presented a nonlocal shear deformation beam theory for bending, buckling, and vibration of FG nanobeams using the nonlocal differential constitutive relations of Eringen. Bounouara *et al*. (2016) presented a zeroth-order shear deformation theory for free vibration analysis of FG nanoscale plates resting on elastic foundation. Ahouel *et al*. (2016) developed a nonlocal trigonometric shear deformation beam theory based on neutral surface position for bending, buckling, and vibration of FG nanobeams using the nonlocal differential constitutive relations of Eringen. Chaht *et al*. (2015) studied the bending and buckling behaviors of size- dependent nanobeams made of FGMs including the thickness stretching effect. Al-Basyouni *et al*. (2015) proposed an unified beam formulation and a modified couple stress theory that considered a variable length scale parameter in conjunction with the neutral axis concept to study bending and dynamic behaviors of FG micro beam. Matsunaga (1996-1999) analyzed the natural frequencies and buckling of deep isotropic beams subjected to axial stress by using the approximate one-dimensional higher-order theories.
Nguyen *et al*. (2014) present an analytical solution for the size-dependent static analysis of the functionally graded (FG) nanobeams with various boundary conditions based on the nonlocal continuum model. Thai *et al*. (2017) presented a numerical model for the bending, buckling and free vibration analyses of FG microplates. The size-dependent effect was captured by using the modified strain gradient elasticity theory with three length scale parameters, whilst the shear deformation effect was accounted by using the third-order shear deformation theory. Thai *et al*. (2017) used the isogeometric analysis to investigate the post-buckling behavior of FG microplates subjected to mechanical and thermal loads. The modified a strain gradient theory with three length scale parameters was used to capture the size effect. Nguyen *et al*. (2015) proposed an efficient computational approach based on refined plate theory including the thickness stretching effect in conjunction with isogeometric formulation for the size-dependent bending, free vibration and buckling analysis of FG nanoplate structures. Trinh (2016) investigated the mechanical behaviours of FG microbeams based on the modified couple stress theory. The material properties of these beams were varied through beam's depth and calculated by using classical rule of mixture and Mori–Tanaka scheme. Trinh (2017) presented the static bending, free vibration and buckling behaviours of FG sandwich microplates under mechanical and thermal loads. Governing equations of both higher-order shear deformation and quasi-3D theories were derived based on the variational principle and modified couple stress theory. Trinh (2018) studied the free vibration behaviour of bi-dimensional FG microbeams under arbitrary boundary conditions. Based on the frame work of the modified couple stress theory and Hamilton's principle, governing equations of motion were developed for the bi-dimensional FG microbeams using a quasi-3D theory. A new nonlocal hyperbolic refined plate model for free vibration properties of functionally graded (FG) plates was presented by (Belkorissat *et al*. 2015a, b). This nonlocal nano-plate model incorporates the length scale parameter, which can capture the small-scale effect. (Tebboune *et al*. 2015a, b) presented a trigonometric shear deformation theory for thermal buckling analysis of functionally graded plates. The theory accounts for sinusoidal distribution of transverse shear stress, and satisfies the free transverse shear stress conditions on the top and bottom surfaces of the plate without using shear correction factor. Bourada *et al*. (2015) developed a refined trigonometric higher-order beam theory for bending and vibration of functionally graded beams. In this theory, in addition to modeling the displacement field, the thickness stretching effect is also included. Hebali *et al*. (2014) developed a quasi-three-dimensional (3D) hyperbolic shear deformation theory for the bending and free vibration analysis of functionally graded plates. Unlike any other theory, the number of unknown functions involved in displacement field is only five, as against six or more in the case of other shear and normal deformation theories. Bennoun *et al*. (2016) developed a new five-variable refined plate theory for the free vibration analysis of functionally graded sandwich plates. Bousahla *et al*. (2016) presented a four-variable refined plate theory for buckling analysis of functionally graded plates subjected to uniform, linear and non-linear temperature rises across the thickness direction. Belabed *et al*. (2014) presented an efficient and simple higher order shear and normal deformation theory for functionally graded material (FGM) plates. By dividing the transverse displacement into bending, shear and

thickness stretching parts, the number of unknowns and governing equations for the present theory is reduced. Surface stress and surface elasticity have been accepted as important factors that may clarify the experimentally measured size dependent elastic modulus of nanobeams. Some analytical methods have been suggested to integrate these surface effects into the Euler-Bernoulli law for elementary beam theory to examine the elastic behavior of nanobeams. According to the performed researches and corresponding results, a gap exists in open literature that is, study the surface effect via high order theory. This paper aims to fill the gap. In the present paper the buckling and transverse vibration of nanobeams under uniaxial load were studied based on various refined higher-order shear deformation beam theories. The aim is to investigate accurately the effect of geometrical properties such as thickness and length-to-thickness ratio of the nanobeams when compared to the solutions published in the literature.

2. Governing equations

Consider a beam with length L and rectangular cross-section b×h, where b is the width and h is the height, as Fig. 1 shows. In this figure, (x, y, z) coordinates represent the length, width, and height of the beam. The formulation is limited to linear elastic material behavior. The displacement fields of various shear deformation beam theories are selected based on the following assumptions: (1) the axial and transverse displacements are partitioned into bending and shear components, respectively; (2) the bending component of the axial displacement is similar to that given by the classical beam theory (CBT); and (3) the shear component of the axial displacement gives rise to the higher-order variation of shear strain and, hence, to shear stress through the depth of the beam in such a way that shear stress vanishes on the top and bottom surfaces. Based on these assumptions, the displacement fields of various higher-order shear deformation beam theories are given in a general form as follows:

$$u_x(\mathrm{x},\mathrm{z}) = u(\mathrm{x}) - z\frac{\partial w_b}{\partial x} - f(\mathrm{z})\frac{\partial w_s}{\partial x}$$
$$u_y(\mathrm{x},\mathrm{z}) = 0 \qquad (1)$$
$$u_z(\mathrm{x},\mathrm{z}) = w_b(\mathrm{x}) + w_s(\mathrm{x})$$

where (u_x, u_z) are the axial displacement and the transverse displacement of points of the beam, w_b and w_s are the bending and shear components of transverse displacement of a point on the mid-plane of the beam, respectively, and f(z) is a shape function determining the distribution of the transverse shear strain and shear stress through the depth of the beam. The shape function f(z) is selected to satisfy the stress-free boundary conditions on the top and bottom surfaces of the beam; thus a shear correction factor is not required. Boukhari *et al*. (2016) developed a shear deformation theory for wave propagation analysis of an infinite FG plate in the presence of thermal environments.

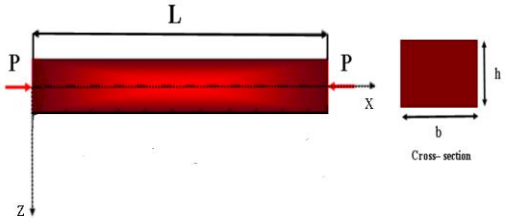

Fig. 1 Geometry and coordinate of a nanobeam with rectangular cross-section under axial load

By dividing the transverse displacement into bending and shear parts, the number of unknowns and governing equations of the present theory was reduced. Ait Yahia *et al*. (2015) developed various higher-order shear deformation plate theories for wave propagation in FG plates having porosities. Bouderba *et al*. (2016) developed a first-order shear deformation theory to analysis the thermal buckling response of FG sandwich plates. Bousahla *et al*. (2016) presented a four-variable refined plate theory for buckling analysis of FG plates subjected to uniform, linear and non-linear temperature rises across the thickness direction. Beldjelili *et al*. (2016) discussed the hygro-thermo-mechanical bending behavior of sigmoid FG plate resting on variable two-parameter elastic foundations using a four-variable refined plate theory. Tounsi *et al*. (2013) presented a refined trigonometric shear deformation theory taking into account transverse shear deformation effects for the thermoelastic bending analysis of FG sandwich plates. Saidi (2016) proposed an hyperbolic shear deformation theory for vibration analysis of thick FG rectangular plates resting on elastic foundations. The displacement fields of the third-order beam theory (TBT) based on Reddy (1984), sinusoidal beam theory (SBT) based on Touratier (1991), hyperbolic beam theory (HBT) based on Soldatos (1992), and exponential beam theory (EBT) based on Karama *et al*. (2003) can be obtained from Eq. (1) by using different shape functions f(z) given in Table 1. It is noted that the displacement fields of the proposed theories are different from those of the existing higher-order theories such as TBT (1984), SBT (1991), HBT (1992), and EBT (2003). In the proposed theories, the transverse displacement u_z is partitioned into the bending and shear parts components (see Eq. (1)), whereas the transverse displacement of the above-mentioned theories is not partitioned into the bending and shear parts. The partition of the transverse displacement into the bending and shear parts helps identify the contributions of shear parts and bending to the total transverse displacement. The non-zero strains read:

$$\varepsilon_{xx} = \frac{\partial u}{\partial x} - z\frac{\partial^2 w_b}{\partial x^2} - f\frac{\partial^2 w_s}{\partial x^2} \qquad (2)$$

$$\gamma_{xz} = \left(1 - \frac{\partial f}{\partial z}\right)\frac{\partial w_s}{\partial x} \equiv g\frac{\partial w_s}{\partial x} \qquad (3)$$

where $g(z)=\left(1-\partial f / \partial z\right)$ are the shape functions of the transverse shear strains given in Table 1, for various beam models. These shape functions represent the distribution of the transverse shear strains and, hence, the transverse shear stresses through the depth of the beam.

Table 1 Shape functions

Model	$f(z)$	$g(z)=1-df/dz$
TBT based on Reddy	$\frac{4z^3}{3h^2}$	$1-\frac{4z^2}{h^2}$
SBT Touratier	$z-\frac{h}{\pi}\sin(\frac{\pi z}{h})$	$\cos(\frac{\pi z}{h})$
HBT based on Soldates	$z-h\sinh(\frac{z}{h})+z\cosh(\frac{1}{2})$	$\cosh(\frac{z}{h})-\cosh(\frac{1}{2})$
EBT based on Karama *et al*	$z-ze^{-2(z/h)^2}$	$\left(1-\frac{4z^2}{h^2}\right)e^{-2(z/h)^2}$
Classic Beam Theory (CBT)	z	0

3. Surface elasticity and its influence on beam deformation

The increasing contribution of surface properties is believed to be the main reason for the effect of size on materials. In fact, the effect of size on the mechanical properties of materials is analyzed primarily within the framework of surface effects. The surface atoms have a lower co-ordination number compared to the bulk atoms, i.e. they have fewer neighbors (Sun *et al*. 2002a, b). As a result, the charge density in the vicinity of the surface is redistributed. Correspondingly, the nature of the chemical bond and the equilibrium interatomic distances on the surface are different from those inside the bulk (Haiss 2001). Researchers have studied the effects of surface on nanoscale materials such as nanoplates, nanowires, and nanorods (Miller and Shenoy 2000, Dingreville and Cherkaoui 2005, He *et al*. 2004, Shenoy 2002, Shenoy 2005, Sharma *et al*. 2003). The effects of surface on the mechanical behavior of nanomaterials can be examined by considering surface energy and/or surface stresses. According to Gibbs (1906) and Cammarata (1994), the surface stress tensor $\sigma^s_{\alpha\beta}$ is related to the surface energy density γ through the surface strain tensor $\varepsilon^s_{\alpha\beta}$ by:

$$\sigma^s_{\alpha\beta}=\gamma\delta_{\alpha\beta}+\frac{\partial\gamma}{\partial\varepsilon^s_{\alpha\beta}} \tag{4}$$

The one-dimensional and linear relationships of the stress-strain of equation (4) are used as follows:

$$\sigma^s=\tau^0+E^s\varepsilon \tag{5}$$

where τ^0 is the residual surface tension under unstrained condition, and E^s is the surface elastic modulus, which can be determined by atomistic simulations or experiments (Jing *et al*. 2006a, b, Miller and Shenoy 2000).

4. Equations of motion

The governing equations and the boundary conditions will be obtained by using the principle of the minimum total potential energy. The first variation of the strain energy is indicated as follows:

$$\begin{aligned}\delta U&=\int_0^L\int_A\left(\sigma_x\delta\varepsilon_x+\sigma_{xz}\delta\gamma_{xz}\right)\,dAdx\\&=\int_0^l\left(N\frac{d\delta u}{dx}-M_b\frac{d^2\delta w_b}{dx^2}-M_s\frac{d^2\delta w_s}{dx^2}+Q\frac{d\delta w_s}{dx}\right)dx\end{aligned} \tag{6}$$

where δU is the virtual variation of the strain energy, and *N*, *M*, and Q are the stress resultants that are defined for use in the next sections as:

$$\begin{aligned}&N=\int_A\sigma_{xx}dA,\quad M_s=\int_A f\sigma_{xx}dA,\\&M_b=\int_A z\sigma_{xx}dA,\quad Q=\int_A g\sigma_{xz}dA\end{aligned} \tag{7}$$

The variation of the potential energy by the transverse load q applied and the axial compressive load p can be written as:

$$\begin{aligned}\delta V=&-\int_0^L q\,\delta\left(w_b+w_s\right)d\,x-\\&\int_0^L p\frac{d\left(w_b+w_s\right)}{dx}\frac{d\delta\left(w_b+w_s\right)}{dx}d\,x\end{aligned} \tag{8}$$

El-Haina *et al*. (2017) presented an analytical approach to investigate the thermal buckling behavior of thick FG sandwich by employing both the sinusoidal shear deformation theory and stress function. Menasria *et al*. (2017) suggested an higher shear deformation theory to analyze the thermal buckling response of FG sandwich plates. Abualnour *et al*. (2018) presented a shear deformation theory including the stretching effect for free vibration of the simply supported FG plates. Houari *et al*. (2016) developed a higher-order shear deformation theory for bending and free vibration analysis of functionally graded (FG) plates. The variation of the kinetic energy can be expressed as:

$$\begin{aligned}\delta K&=-\int_0^L\int_A\rho(z)\left(\dot{u}_1\,\delta\dot{u}_1+\dot{u}_3\,\delta\dot{u}_3\right)dAdx\\&=-\int_0^L\left\{I_0\left[\dot{u}\,\delta\dot{u}+\left(\dot{w}_b+\dot{w}_s\right)\delta\left(\dot{w}_b+\dot{w}_s\right)\right]\right.\\&\left.+I_1\frac{d\,\dot{w}_b}{dx}\frac{d\delta\,\dot{w}_b}{dx}+K_1\frac{d\,\dot{w}_s}{dx}\frac{d\delta\,\dot{w}_s}{dx}\right\}dx\end{aligned} \tag{9}$$

where dot-superscript convent illustrates the differentiation with regard to the time variable t, $\rho(z)$ is the mass density, and (I_0, I_1, K_1) are the mass inertias determined as

$$\begin{aligned}&I_0=\int_A\rho(z)\,dA,\\&I_1=\int_A z^2\rho(z)\,dA,\\&K_1=\int_A f^2\rho(z)\,dA\end{aligned} \tag{10}$$

Hamilton's principle is used herein to derive the equations of motion. The principle can be stated in an analytical form as (Reddy 2002):

$$\int_0^T\left(\delta U+\delta V-\delta K\right)dt=0 \tag{11}$$

where substituting the expressions for δU, δV and δK from Eqs. (6)-(8) and Eq. (9) into Eq. (11) leads to:

$$\begin{aligned}&\int_0^T\left\{\int_0^l\left(N\frac{d\delta u}{dx}-M_b\frac{d^2\delta w_b}{dx^2}-M_s\frac{d^2\delta w_s}{dx^2}+Q\frac{d\delta w_s}{dx}\right)dx\right.\\&-\int_0^L q\delta\left(w_b+w_s\right)dx\\&-\int_0^L p\frac{d\left(w_b+w_s\right)}{dx}\frac{d\delta\left(w_b+w_s\right)}{dx}dx\\&\left.+\int_0^L\left\{I_0\left[\dot{u}\,\delta\dot{u}+\left(\dot{w}_b+\dot{w}_s\right)\delta\left(\dot{w}_b+\dot{w}_s\right)\right]\right.\right.\\&\left.\left.+I_1\frac{d\dot{w}_b}{dx}\frac{d\delta\dot{w}_b}{dx}+K_1\frac{d\dot{w}_s}{dx}\frac{d\delta\dot{w}_s}{dx}\right\}dx\right\}dt=0\end{aligned}\tag{12}$$

After integrating by parts versus both space and time variables and collecting the coefficients of δu, δw_b, and δw_s, the following equations of motion of the beam are achieved:

$$\delta u:\frac{\partial N}{\partial x}=I_0\ddot{u}\tag{13}$$

$$\begin{aligned}\delta w_b:\ &\frac{\partial^2 M_b}{\partial x^2}+q-p\frac{d^2\left(w_b+w_s\right)}{dx^2}\\&=I_0\left(\ddot{w}_b+\ddot{w}_s\right)-I_1\frac{\partial^2\ddot{w}_b}{\partial x^2}\end{aligned}\tag{14}$$

$$\begin{aligned}\delta w_s:\ &\frac{\partial^2 M_s}{\partial x^2}+\frac{\partial Q}{\partial x}+q-p\frac{d^2\left(w_b+w_s\right)}{dx^2}\\&=I_0\left(\ddot{w}_b+\ddot{w}_s\right)-K_1\frac{\partial^2\ddot{w}_s}{\partial x^2}\end{aligned}\tag{15}$$

The boundary conditions are of the form:

$$N=0\ \text{ or }\ u=0\tag{16a}$$

$$Q_b\equiv\frac{dM_b}{dx}-p\frac{d\left(w_b+w_s\right)}{dx}+I_1\frac{d\ddot{w}_b}{dx}\ \text{ or }\ w_b=0\tag{16b}$$

$$Q_s\equiv\frac{dM_s}{dx}+Q-p\frac{d\left(w_b+w_s\right)}{dx}+K_1\frac{d\ddot{w}_s}{dx}\ \text{ or }\ w_s=0\tag{16c}$$

$$M_b=0\ \text{ or }\ \frac{dw_b}{dx}=0\tag{16d}$$

$$M_s=0\ \text{ or }\ \frac{dw_s}{dx}=0\tag{16e}$$

The equations of motion and boundary conditions of the CBT can be achieved from Eqs. (14)-(15) by setting the shear component of transverse displacement w_s equal to zero. The linear constitutive relations of a beam are given as (Thai and Vo 2012):

$$\begin{aligned}&\sigma_{xz}=Q_{55}\gamma_{xz},\ Q_{55}=\frac{E}{2\left(1+\upsilon\right)}\\&\sigma_x=Q_{11}\varepsilon_x,\quad Q_{11}=E\end{aligned}\tag{17}$$

After substituting Eqs. (4)-(5) into Eq. (17) and the subsequent results into Eq. (7), the constitutive equations for the stress resultants are obtained as follows:

$$\begin{aligned}&N=EA\frac{du}{dx},\ M_b=-ED\frac{d^2w_b}{dx^2}\\&M_S=-EH_s\frac{d^2w_s}{dx^2},\ Q=A_S\frac{dw_s}{dx}\end{aligned}\tag{18}$$

$$A=\int_A dA,\ \ B=\int_A zdA,\ B_s=\int_A f\,dA,\ D=\int_A z^2dA,$$

$$D_s=\int_A zf\,dA,\ H_s=\int_A f^2dA,\ A_s=\int_A g^2Q_{55}dA\tag{19}$$

5. Equations of motion in terms of displacement

The governing equations of motion in terms of displacements u, w_b and w_s can be obtained by substituting the stress resultants in Eq. (18) into Eqs. (13) to (15), leading to:

$$EA\frac{d^2u}{dx^2}=I_0\ddot{u}\tag{20}$$

$$\begin{aligned}&-ED\frac{d^4w_b}{dx^4}-ED_s\frac{d^4w_s}{dx^4}+q\\&-p\frac{d^2\left(w_b+w_s\right)}{dx^2}=I_0\left(\ddot{w}_b+\ddot{w}_s\right)-I_1\frac{\partial^2\ddot{w}_b}{\partial x^2}\end{aligned}\tag{21}$$

$$\begin{aligned}&-ED_s\frac{d^4w_b}{dx^4}-EH_s\frac{d^4w_s}{dx^4}+A_s\frac{d^2w_s}{dx^2}\\&+q-p\frac{d^2\left(w_b+w_s\right)}{dx^2}\\&=I_0\left(\ddot{w}_b+\ddot{w}_s\right)-K_1\frac{\partial^2\ddot{w}_s}{\partial x^2}\end{aligned}\tag{22}$$

The residual surface tension will create a distributed loading $q(x)$ along the transverse direction as follows:

$$q\left(x\right)=H\frac{d^2\left(w_b+w_s\right)}{dx^2}\tag{23}$$

where the parameter H is a constant determined by the remaining surface tension and the shape of cross-section. For rectangular cross-section, H is given, separately, by:

$$H=2b\,\tau_0\tag{24}$$

where τ_0 is the residual surface tension (Wang and Feng 2009). Therefore, substituting Eq. (23) in Eq. (21) into (22) leads to the following equilibrium equation

$$\begin{aligned}&-ED\frac{d^4w_b}{dx^4}-ED_s\frac{d^4w_s}{dx^4}+H\frac{d^2\left(w_b+w_s\right)}{dx^2}\\&-p\frac{d^2\left(w_b+w_s\right)}{dx^2}=I_0\left(\ddot{w}_b+\ddot{w}_s\right)-I_1\frac{\partial^2\ddot{w}_b}{\partial x^2}\end{aligned}\tag{25}$$

$$-ED_s\frac{d^4w_b}{dx^4}-EH_s\frac{d^4w_s}{dx^4}+A_s\frac{d^2w_s}{dx^2}+H\frac{d\ \left(w_b+w_s\right)}{dx^2}-p\frac{d^2\left(w_b+w_s\right)}{dx^2}=I_0\left(\ddot{w}_b+\ddot{w}_s\right)-K_1\frac{\partial^2\ddot{w}_s}{\partial x^2} \tag{26}$$

In conclusion, the critical buckling load and free vibration of nanobeam for various higher-order shear deformation beam theories are obtained by the following equation:

$$D_{11}\frac{d^4w_b}{dx^4}+D_{12}\frac{d^4w_s}{dx^4}-H\frac{d^2\left(w_b+w_s\right)}{dx^2}+p\frac{d^2\left(w_b+w_s\right)}{dx^2}=-I_0\left(\ddot{w}_b+\ddot{w}_s\right)+I_1\frac{\partial^2\ddot{w}_b}{\partial x^2} \tag{27}$$

$$D_{12}\frac{d^4w_b}{dx^4}+D_{22}\frac{d^4w_s}{dx^4}-A_s\frac{d^2w_s}{dx^2}-H\frac{d^2\left(w_b+w_s\right)}{dx^2}+p\frac{d^2\left(w_b+w_s\right)}{dx^2}=-I_0\left(\ddot{w}_b+\ddot{w}_s\right)+K_1\frac{\partial^2\ddot{w}_s}{\partial x^2} \tag{28}$$

A nanobeam with rectangular cross-section D is obtained as follows:

$$D_{11}=\left(D\frac{12EI}{h^3}\right) \tag{29}$$

$$D_{12}=\left(D_s\frac{12EI}{h^3}\right) \tag{30}$$

$$D_{22}=\left(H_s\frac{12EI}{h^3}\right) \tag{31}$$

In the case of a rectangular cross-section nanobeam, *EI* is presented as (Wang and Feng 2009):

$$EI=E\frac{wh^3}{12} \tag{32}$$

where *E* is the Young's modulus. Moreover, *w* and *h* are the width and height of a rectangle cross-section of a nanobeam, respectively. The influence of surface elasticity can be exerted on the buckling and free vibration of a nanobeam by changing the traditional flexural rigidity *EI* for the bulk material by EI^* where is the effective flexural rigidity, which consists of the surface bending elasticity on the nanobeam with rectangular cross-section, which is given by (Wang and Feng 2009):

$$EI^*=EI+(\frac{1}{2}E^sb\,h^2)+(\frac{1}{6}E^sh^3) \tag{33}$$

where

$$D_{11}^*=\left(D\frac{12EI^*}{h^3}\right) \tag{34}$$

$$D_{12}^*=\left(D_s\frac{12EI^*}{h^3}\right) \tag{35}$$

$$D_{22}^*=\left(H_s\frac{12EI^*}{h^3}\right) \tag{36}$$

Consequently, substituting Eqs. (34) to (36) into Eqs. (27) to (28) leads to the following equilibrium equations for a nanobeam with surface effect

$$D_{11}^*\frac{d^4w_b}{dx^4}+D_{12}^*\frac{d^4w_s}{dx^4}-H\frac{d^2\left(w_b+w_s\right)}{dx^2}+p\frac{d^2\left(w_b+w_s\right)}{dx^2}=-I_0\left(\ddot{w}_b+\ddot{w}_s\right)+I_1\frac{\partial^2\ddot{w}_b}{\partial x^2} \tag{37}$$

$$D_{12}^*\frac{d^4w_b}{dx^4}+D_{22}^*\frac{d^4w_s}{dx^4}-A_s\frac{d^2w_s}{dx^2}-H\frac{d^2\left(w_b+w_s\right)}{dx^2}+p\frac{d^2\left(w_b+w_s\right)}{dx^2}=-I_0\left(\ddot{w}_b+\ddot{w}_s\right)+K_1\frac{\partial^2\ddot{w}_s}{\partial x^2} \tag{38}$$

5. Analytical solutions of buckling and free vibration of nanobeams

In this part, the governing equations are analytically solved for the buckling and free vibration of a nanobeam. The Navier solution method is employed to obtain the analytical solutions for the simply supported boundary conditions. In the future, the researchers can also extend this model for nanobeams with other boundary conditions. Furthermore, the following natural boundary conditions at $x=0,\mathrm{L}$ are achieved:

$$w_b=w_s=M_b=M_s=0\quad at\quad x=0,L \tag{39}$$

The following expansions of the displacements *w(x)* yield the boundary conditions in Eq. (39) for the free vibration:

$$w_b\left(x,t\right)=\sum_{n=1}^{\infty}W_{bn}\,sin\left(\frac{n\pi x}{L}\right)e^{iw_nt} \tag{40}$$

$$w_s\left(x,t\right)=\sum_{n=1}^{\infty}W_{sn}\,sin\left(\frac{n\pi x}{L}\right)e^{iw_nt} \tag{41}$$

When *t= 0*, the solution is assumed for any n for the buckling:

$$w\left(x,0\right)=\sum_{n=1}^{\infty}W_n\,\sin\left(\frac{n\pi x}{l}\right) \tag{42}$$

Consequently, the explicit buckling load and free vibration of the nanobeams can be easily obtained by

$$\begin{aligned}&\left(D_{11}^{*}\alpha^4+H\alpha^2\right)W_b\sin\alpha+\left(D_{12}^{*}\alpha^4+H\alpha^2\right)W\sin\alpha_s\\&-p\alpha^2W_b\sin\alpha-p\alpha^2W_s\sin\alpha\\&=I_0\left(\omega_n^2W_b\sin\alpha+\omega_n^2W_s\sin\alpha\right)+I_1\alpha^2\omega_n^2W_b\sin\alpha\end{aligned}\tag{43}$$

$$\begin{aligned}&\left(D_{12}^{*}\alpha^4+H\alpha^2\right)W_b\sin\alpha+\\&\left(D_{22}^{*}\alpha^4+A_s\alpha^2+H\alpha^2\right)W_s\sin\alpha\\&-p\alpha^2W_b\sin\alpha-p\alpha^2W_s\sin\alpha\\&=I_0\left(\omega_n^2W_b\sin\alpha+\omega_n^2W_s\sin\alpha\right)\\&+K_1\alpha^2\omega_n^2W_b\sin\alpha\end{aligned}\tag{44}$$

This leads to:

$$\begin{aligned}&\left(D_{11}^{*}\alpha^4+H\alpha^2\right)W_b+\left(D_{12}^{*}\alpha^4+H\alpha^2\right)W_s\\&-p\alpha^2W_b-p\alpha^2W_s-\left(I_0+I_1\alpha^2\right)\omega_n^2W_b\\&-I_0\omega_n^2W_s=0\end{aligned}\tag{45}$$

$$\begin{aligned}&\left(D_{12}^{*}\alpha^4+H\alpha^2\right)W_b+\left(D_{22}^{*}\alpha^4+A_s\alpha^2+H\alpha^2\right)W_s\\&-p\alpha^2W_b-p\alpha^2W_s\\&-\left(I_0+K_1\alpha^2\right)\omega_n^2W_b-I_0\omega_n^2W_s=0\end{aligned}\tag{46}$$

If

$$\begin{aligned}S_{11}&=\left(D_{11}^{*}\alpha^4+H\alpha^2\right),\\S_{12}&=\left(D_{12}^{*}\alpha^4+H\alpha^2\right),\\S_{22}&=\left(D_{22}^{*}\alpha^4+A_s\alpha^2+H\alpha^2\right)\end{aligned}\tag{47}$$

$$m_{11}=\left(I_0+I_1\alpha^2\right),\quad m_{12}=I_0,\quad m_{22}=\left(I_0+K_1\alpha^2\right)$$

we have

$$\begin{aligned}&\left(\begin{bmatrix}S_{11}&S_{12}\\S_{12}&S_{22}\end{bmatrix}-p\alpha^2\begin{bmatrix}1&1\\1&1\end{bmatrix}-\omega_n^2\begin{bmatrix}m_{11}&m_{12}\\m_{12}&m_{22}\end{bmatrix}\right)\\&\begin{Bmatrix}W_{bn}\\W_{sn}\end{Bmatrix}=\begin{Bmatrix}0\\0\end{Bmatrix}\end{aligned}\tag{48}$$

To conclude, the critical buckling load is obtained from Eq. (48) by following the same procedure as solution of Eq. (48) as:

$$\omega_n=0,\qquad p_{cr}=\frac{1}{\alpha^2}\left(\frac{S_{12}^2-S_{11}S_{22}}{2S_{12}-S_{11}-S_{22}}\right)\tag{49}$$

To conclude, in what follows, the free vibration is obtained from Eq. (48) by following the same procedure as the solution of Eq. (48):

$$p=0,\qquad \omega_{cr}=\sqrt{\frac{\left(-S_{11}m_{22}-S_{22}m_{11}+\left(2S_{12}m_{12}\right)\right)+\sqrt{\left(-S_{11}m_{22}-S_{22}m_{11}+\left(2S_{12}m_{12}\right)\right)^2-4\left(\left(m_{12}\right)^2-m_{11}m_{22}\right)\left(S_{11}S_{22}-\left(S_{12}\right)^2\right)}}{2\left(\left(m_{12}\right)^2-m_{11}m_{22}\right)}}\tag{50}$$

The buckling of nanobeams by Euler beam theory with surface effects is derived as (Wang and Feng 2009):

$$p_{cr0}=\frac{\left(\mathrm{EI}^{*}\left(\frac{n\pi}{l}\right)^2+H\right)}{\left(\frac{n\pi}{l}\right)^2\mathrm{EI}}\tag{51}$$

Additionally, the vibration of nanobeams by Euler beam theory with surface effects is derived as (Wang and Feng 2009):

$$\omega_{cr0}=\sqrt{\left(1+\frac{H}{\left(\frac{n\pi}{l}\right)^2\mathrm{EI}^{*}}\right)\left(1+\frac{\mathrm{EI}^{*}-\mathrm{EI}}{\mathrm{EI}}\right)}\tag{52}$$

7. Numerical results and discussion

In this section, several numerical examples are presented and discussed to validate the accuracy of the present nanobeam models in predicting the nanobeam stability. As an example, in what follows, we consider a nanobeam with rectangular cross-section:

The material constants are considered to be E=76 GPa, τ^0=0.89 N/m, and E^s=1.22 GPa on the surface of a nanobeam made of silver.

Tables 2 to 4 show the change in the critical buckling load (P_{cr} / P_{cr0}). Tables 5 to 7 show the change in the normalized critical frequency (ω_{cr} /ω_{cr0}) for different length-to-thickness ratios and mode numbers (n = 1, 2, 3). For higher-order theory of the third degree, the sinusoidal and exponential higher-order theories with a simply supported nanobeam are calculated to ensure the accuracy of the calculations by comparing the results with those in Ref. (Wang and Feng 2009). The results are in a good agreement with those in the reference resources. It is also necessary to mention that many of these analyses are taken into account based on the theory of beams without surface effects. The tables show that the critical buckling load and the normalized critical frequency for very small length-to-thickness ratio here (l<5h) are less than high length-to-thickness ratio. This also accounts for the fact that size has an important effect on the critical buckling load and the normalized critical frequency when the beam is very small and is at the nanometer scale. As observed here, in these theories, the critical buckling load and the normalized critical frequency decrease by increasing the thickness. Additionally, it can be concluded that the critical buckling load and the normalized critical frequency for higher-order theory of the third degree are greater than those in sinusoidal and exponential higher-order theories.

Fig. 2 shows the critical buckling under axial compressive load by considering surface effect on the length-to-thickness ratio for different theories. The results presented in this figure reveal that the critical buckling load for higher-order theory of the third degree is greater than that of the sinusoidal and exponential higher-order theories. In addition, as the thickness increases, the critical buckling load for higher-order theory is reduced. In lower thickness, the critical buckling load for exponential higher-order theory has the highest decrease.

Table 2 Critical compressive load of a nanobeam as a function of (L/h) for various modes (h= 10nm, E=76 Gpa)

n	Method	$L/h=5$	$L/h=10$	$L/h=20$	$L/h=100$
1	Wang *et al* (2009)	1.08082	1.29440	2.14869	29.4862
	TBT	1.08481	1.30126	2.15592	29.4935
	SBT	1.08442	1.30122	2.15590	29.4935
	EBT	1.08400	1.30115	2.15587	29.4935
2	Wang *et al* (2009)	1.02743	1.08082	1.29440	8.12878
	TBT	1.00537	1.08481	1.30126	8.13607
	SBT	1.00156	1.08442	1.30122	8.13606
	EBT	0.99768	1.08400	1.30115	8.13603
3	Wang *et al* (2009)	1.01754	1.04127	1.13619	4.17370
	TBT	0.93316	1.03656	1.14212	4.18098
	SBT	0.92224	1.03502	1.14198	4.18096
	EBT	0.91149	1.03342	1.14181	4.18093

Table 3 Critical compressive load of a nanobeam as a function of (L/h) for various modes (h= 20nm, E=76 Gpa)

n	Method	$L/h=5$	$L/h=10$	$L/h=20$	$L/h=100$
1	Wang *et al* (2009)	1.04041	1.14720	1.57435	15.2431
	TBT	1.04130	1.15056	1.57795	15.2468
	SBT	1.04093	1.15052	1.57795	15.2468
	EBT	1.04054	1.15048	1.57793	15.2467
2	Wang *et al* (2009)	1.013710	1.04041	1.14720	4.56439
	TBT	0.989830	1.04130	1.15056	4.56804
	SBT	0.986089	1.04093	1.15052	4.56803
	EBT	0.982288	1.04054	1.15048	4.56801
3	Wang *et al* (2009)	1.008770	1.20640	1.06810	2.58685
	TBT	0.923927	1.01342	1.07069	2.59049
	SBT	0.913125	1.01191	1.07056	2.59048
	EBT	0.902492	1.01036	1.07042	2.59046

Table 4 Critical compressive load of a nanobeam as a function of (L/h) for various modes (h= 10nm, E=76 Gpa)

n	Method	$L/h=5$	$L/h=10$	$L/h=20$	$L/h=100$
1	Wang *et al* (2009)	1.01616	1.05888	1.22974	6.69724
	TBT	1.01519	1.06013	1.23118	6.69870
	SBT	1.01484	1.06010	1.23117	6.69870
	EBT	1.01447	1.06007	1.23116	6.69870
2	Wang *et al* (2009)	1.00549	1.01616	1.05888	2.42576
	TBT	0.98050	1.01519	1.06013	2.42721
	SBT	0.97680	1.01484	1.06010	2.42721
	EBT	0.97304	1.01447	1.06007	2.42721
3	Wang *et al* (2009	1.00351	1.00825	1.02724	1.63474
	TBT	0.91838	0.99953	1.02783	1.63619
	SBT	0.90764	0.99805	1.02771	1.63619
	EBT	0.89708	0.99653	1.02758	1.63618

Table 5 The normalized critical frequency of a nanobeam as a function of (L/h) for various modes (h= 20nm, E=76 Gpa)

n	Method	$L/h=5$	$L/h=10$	$L/h=20$	$L/h=100$
1	Wang *et al* (2009)	1.03963	1.13772	1.46584	5.43012
	TBT	1.04164	1.14073	1.46830	5.43079
	SBT	1.04147	1.14071	1.43830	5.43079
	EBT	1.04128	1.14069	1.46829	5.43079
2	Wang *et al* (2009)	1.03963	1.13772	1.46584	5.43012
	TBT	1.04164	1.14073	1.46830	5.43079
	SBT	1.04147	1.14071	1.43830	5.43079
	EBT	1.04128	1.14069	1.46829	5.43079
3	Wang *et al* (2009)	1.03963	1.13772	1.46584	5.43012
	TBT	1.04164	1.14073	1.46830	5.43079
	SBT	1.04147	1.14071	1.43830	5.43079
	EBT	1.04128	1.14069	1.46829	5.43079

Table 6 The normalized critical frequency of a nanobeam as a function of (L/h) for various modes (h= 20nm, E=76 Gpa)

n	Method	$L/h=5$	$L/h=10$	$L/h=20$	$L/h=100$
1	Wang *et al* (2009)	1.02001	1.07107	1.25473	3.90424
	TBT	1.02052	1.07264	1.25617	3.90471
	SBT	1.02036	1.07263	1.25616	3.90471
	EBT	1.02018	1.07261	1.25616	3.90471
2	Wang *et al* (2009)	1.02001	1.07107	1.25473	3.90424
	TBT	1.02052	1.07264	1.25617	3.90471
	SBT	1.02036	1.07263	1.25616	3.90471
	EBT	1.02018	1.07261	1.25616	3.90471
3	Wang *et al* (2009)	1.02001	1.07107	1.25473	3.90424
	TBT	1.02052	1.07264	1.25617	3.90471
	SBT	1.02036	1.07263	1.25616	3.90471
	EBT	1.02018	1.07261	1.25616	3.90471

Table 7 The normalized critical frequency of a nanobeam as a function of (L/h) for various modes (h= 50nm, E=76 Gpa)

n	Method	$L/h=5$	$L/h=10$	$L/h=20$	$L/h=100$
1	Wang *et al* (2009)	1.00805	1.02902	1.10894	2.58790
	TBT	1.00764	1.02963	1.10958	2.58819
	SBT	1.00748	1.02962	1.10958	2.58819
	EBT	1.00731	1.02960	1.10958	2.58818
2	Wang *et al* (2009)	1.00805	1.02902	1.10894	2.58790
	TBT	1.00764	1.02963	1.10958	2.58819
	SBT	1.00748	1.02962	1.10958	2.58819
	EBT	1.00731	1.07260	1.10958	2.58818
3	Wang *et al.* (2009)	1.00805	1.02902	1.10894	2.58790
	TBT	1.00764	1.02963	1.10958	2.58819
	SBT	1.00748	1.02962	1.10958	2.58819
	EBT	1.00731	1.07260	1.10958	2.58818

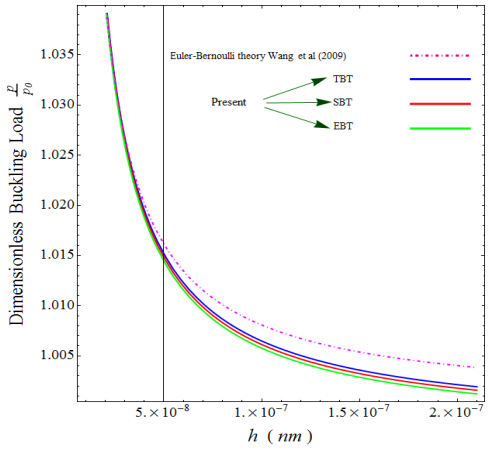

Fig. 2 Critical compressive load of a nanobeam as a function of the thickness (n=1)

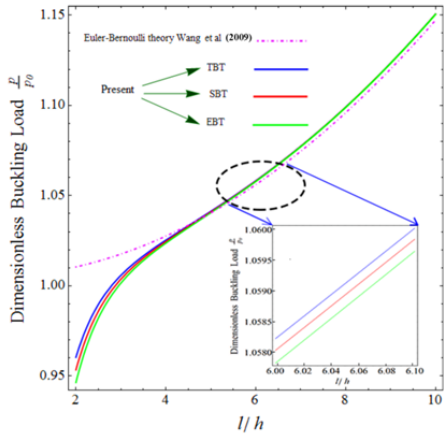

Fig. 3 Critical compressive load of a nanobeam as a function of length-to-thickness ratio (h=20 nm, n=1)

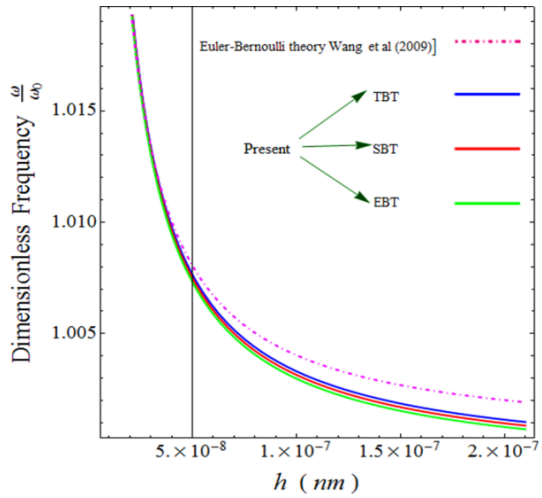

Fig. 4 Normalized critical frequency of a nanobeam as a function of the thickness (n=1)

Fig. 3 shows the critical buckling under axial compressive load by considering the surface effect on the length-to-thickness ratio for different theories. The results presented in this figure indicate that by increasing the length-to-thickness ratio, the critical buckling load increases. The increase in the very small ratio (L/h) is insignificant. Furthermore, as the ratio (L/h) increases, surface effect becomes more significant; for example, for the ratio (L/h=10), the critical buckling load is approximately 1.2 times greater. Moreover, it can be observed that the influence of the surface effect is more considerable as the length decreases in the range of nanometers.

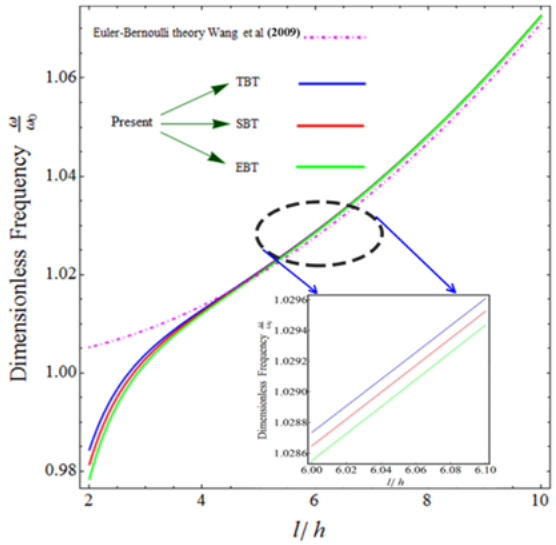

Fig. 5 Normalized critical frequency of a nanobeam as a function of length-to-thickness ratio (h=20 nm, n=1)

Fig. 4 depicts the normalized critical frequency by considering surface effect on the length-to-thickness ratio for different theories. As this figure shows, the critical buckling load for higher-order theory of the third degree is greater than that of the sinusoidal and exponential higher-order theories. Additionally, by increasing the thickness, the normalized critical frequency for higher-order theory is reduced. In other words, in lower thickness, the normalized critical frequency for exponential higher-order theory has the highest decrease.

Fig. 5 shows the normalized critical frequency by considering surface effect on the length-to-thickness ratio

for different theories. The results presented in this figure demonstrate that by increasing the length-to-thickness ratio, the normalized critical frequency increases. The increase in the very small ratio (L/h) is insignificant. As the ratio (L/h) increases, surface effect becomes more considerable; for example, for the ratio (L/h=10), the normalized critical frequency is approximately 1.09 times greater. Furthermore, it can be observed that surface has more substantial effects as the length decreases in the range of nanometers.

5. Conclusions

In this paper, the effect of surface on the buckling and transverse vibration of nanobeams under uniaxial load was studied based on various refined higher-order shear deformation beam theories. The equations of motion were derived using Hamilton's principle, and the buckling and the transverse vibration were obtained by an exact method.

The numerical results showed that surface effect leads to increasing the length-to-thickness ratio, thus increasing the critical buckling load and the normalized critical frequency. Therefore, surface effects play an important role in the buckling and normalized critical frequency responses of the nanobeams. In addition, the results revealed that by increasing the nanobeam thickness, surface exerts greater effects on the critical buckling load and the normalized critical frequency increase for higher-order theory of the third degree compared to the sinusoidal and exponential higher-order theories. The validity of the results obtained was investigated in Tables 1 to 6. According to the increasing ratio of surface area to bulk at nano-scale, surface energy is significantly influential in stubby nanobeams and should be taken into consideration. Accordingly, surface effects should be considered carefully in the analysis of the mechanical behavior of nanostructures.

References

Abdelaziz, H.H., Meziane, M.A.A., Bousahla, A.A., Tounsi, A., Mahmoud, S.R. and Alwabli, A.S. (2017), "An efficient hyperbolic shear deformation theory for bending, buckling and free vibration of FGM sand wich plates with various boundary conditions", *Steel Compos. Struct.*, **25**, 693-704. https://doi.org/10.12989/scs.2017.25.6.693.

Abualnour, M., Houari, M.S.A., Tounsi, A. and Mahmoud, S.R. (2018), "A novel quasi-3D trigonometric plate theory for free vibration analysis of advanced composite plates", *Compos. Struct.*, **184**, 688-697. https://doi.org/10.1016/j.compstruct.2017.10.047.

Ahouel, M., Houari, M. S. A., Bedia, E. A. and Tounsi, A. (2016), "Size-dependent mechanical behavior of functionally graded trigonometric shear deformable nanobeams including neutral surface position concept", *Steel Compos. Struct.*, **20**(5), 963-981. https://doi.org/10.12989/scs.2016.20.5.963.

Al-Basyouni, K. S., Tounsi, A. and Mahmoud, S. R. (2015), "Size dependent bending and vibration analysis of functionally graded micro beams based on modified couple stress theory and neutral surface position", *Compos. Struct.*, **125**, 621-630. https://doi.org/10.1016/j.compstruct.2014.12.070.

Baluch, M. H., Azad, A. K., & Khidir, M. A. (1984), "Technical theory of beams with normal strain", *J. Eng. Mech.*, **110**(8), 1233-1237. https://doi.org/10.1061/(ASCE)0733-9399(1984)110:8(1233).

Belabed, Z., Houari, M. S. A., Tounsi, A., Mahmoud, S. R. and Bég, O. A. (2014), "An efficient and simple higher order shear and normal deformation theory for functionally graded material (FGM) plates", *Compos. Part B Eng.*, **60,** 274-283. https://doi.org/10.1016/j.compositesb.2013.12.057.

Beldjelili, Y., Tounsi, A. and Mahmoud, S. R. (2016), "Hygro-thermo-mechanical bending of S-FGM plates resting on variable elastic foundations using a four-variable trigonometric plate theory", *Smart Struct. Syst.*, **18**(4), 755-786. https://doi.org/10.12989/sss.2016.18.4.755.

Belkorissat, I., Houari, M. S. A., Tounsi, A., Bedia, E. A. and Mahmoud, S. R. (2015), "On vibration properties of functionally graded nano-plate using a new nonlocal refined four variable model", *Steel Compos. Struct.*, **18**(4), 1063-1081. https://doi.org/10.12989/scs.2015.18.4.1063.

Bennoun, M., Houari, M. S. A. and Tounsi, A. (2016), "A novel five-variable refined plate theory for vibration analysis of functionally graded sandwich plates", *Mech. Adv. Mater. Struct.*, **23**(4), 423-431. https://doi.org/10.1080/15376494.2014.984088.

Bhimaraddi, A. and Chandrashekhara, K. (1993), "Observations on higher-order beam theory", *J. Aerosp. Eng.*, **6**(4), 408-413. https://doi.org/10.1061/(ASCE)0893-1321(1993)6:4(408).

Bickford. W.B. (1982), "A consistent higher order beam theory", *Dev. Theoretical Appl. Mech.*, SECTAM, **11**, 137–150, 1982. http://pascal-francis.inist.fr/vibad/index.php?action=getRecordDetail&idt=PASCAL83X0184967.

Bouafia, K., Kaci, A., Houari, M. S. A., Benzair, A. and Tounsi, A. (2017), "A nonlocal quasi-3D theory for bending and free flexural vibration behaviors of functionally graded nanobeams", *Smart Struct. Syst.*, **19**(2), 115-126. https://doi.org/10.12989/sss.2017.19.2.115.

Bouderba, B., Houari, M. S. A., Tounsi, A. and Mahmoud, S. R. (2016), "Thermal stability of functionally graded sandwich plates using a simple shear deformation theory", *Struct. Eng. Mech.*, **58**(3), 397-422. https://doi.org/10.12989/sem.2016.58.3.397.

Boukhari, A., Atmane, H. A., Tounsi, A., Adda, B. and Mahmoud, S. R. (2016), "An efficient shear deformation theory for wave propagation of functionally graded material plates", *Struct. Eng. Mech.*, **57**(5), 837-859. https://doi.org/10.12989/sem.2016.57.5.837.

Bounouara, F., Benrahou, K. H., Belkorissat, I. and Tounsi, A. (2016), "A nonlocal zeroth-order shear deformation theory for free vibration of functionally graded nanoscale plates resting on elastic foundation", *Steel Compos. Struct.*, **20**(2), 227-249. https://doi.org/10.12989/scs.2016.20.2.227.

Bourada, M., Kaci, A., Houari, M. S. A. and Tounsi, A. (2015), "A new simple shear and normal deformations theory for functionally graded beams", *Steel Compos. Struct.*, **18**(2), 409-423. https://doi.org/10.12989/scs.2015.18.2.409.

Bousahla, A. A., Benyoucef, S., Tounsi, A. and Mahmoud, S. R. (2016), "On thermal stability of plates with functionally graded coefficient of thermal expansion", *Struct. Eng. Mech.*, **60**(2), 313-335. https://doi.org/10.12989/sem.2016.60.2.313.

Cammarata, R.C. and Sieradzki, K. (1994), "Surface and interface stresses", *Annual Rev. Mater. Sci.*, **24**(1), 215-234. https://doi.org/10.1146/annurev.pc.45.100194.001045.

Chaht, F. L., Kaci, A., Houari, M.S.A., Tounsi, A., Bég, O. A. and Mahmoud, S.R. (2015), "Bending and buckling analyses of functionally graded material (FGM) size-dependent nanoscale beams including the thickness stretching effect", *Steel Compos. Struct.*, **18**(2), 425-442. https://doi.org/10.12989/scs.2015.18.2.425.

Challamel, N. (2011), "Higher-order shear beam theories and enriched continuum", *Mech. Res. Commun.*, **38**(5), 388-392. https://doi.org/10.1016/j.mechrescom.2011.05.004.

Cowper, G.R. (1966), "The shear coefficient in Timoshenko's beam theory", *Appl. Mech.*, ASME, **33**(2), 335–340, 1966. https://doi.org/10.1115/1.3625046.

Dingreville, R., Qu, J. and Cherkaoui, M. (2005), "Surface free energy and its effect on the elastic behavior of nano-sized particles, wires and films", *J. Mech. Phys. Solids*, **53**(8), 1827-1854. https://doi.org/10.1016/j.jmps.2005.02.012.

Eisenberger, M. (2003), "An exact high order beam element", *Comput. Struct.*, **81**(3), 147-152. https://doi.org/10.1016/S0045-7949(02)00438-8.

El-Haina, F., Bakora, A., Bousahla, A.A., Tounsi, A. and Mahmoud, S.R. (2017), "A simple analytical approach for thermal buckling of thick functionally graded sandwich plates", *Struct. Eng. Mech.,* **63**(5), 585-595. https://doi.org/10.12989/sem.2017.63.5.585.

Ghugal, Y. M. and Sharma, R. (2009), "A hyperbolic shear deformation theory for flexure and vibration of thick isotropic beams", *J. Comput. Methods*, **6**(04), 585-604.

https://doi.org/10.1142/S0219876209002017.
Ghugal, Y. M. and Sharma, R. (2011), "A refined shear deformation theory for flexure of thick beams", *Latin American J. Solids Struct.*, **8**(2), 183-195. https://doi.org/10.1590/S1679-78252011000200005.
Gibbs, J. W. (1906). *The Scientific Papers of J. Willard Gibbs (Vol. 1)*, Longmans, Green and Company., Harlow, United Kingdom.
Gurtin, M. E. and Murdoch, A. I. (1975), "A continuum theory of elastic material surfaces", *Arch. Rational Mech. Anal.*, **57**(4), 291-323. https://doi.org/10.1007/BF00261375.
Haiss, W. (2001), "Surface stress of clean and adsorbate-covered solids", *Reports on Progress in Physics*, **64**(5), 591. https://doi.org/10.1088/0034-4885/64/5/201.
He, L.H., Lim, C.W. and Wu, B.S. (2004), "A continuum model for size-dependent deformation of elastic films of nano-scale thickness", *J. Solids Struct.*, **41**(3-4), 847-857. https://doi.org/10.1016/j.ijsolstr.2003.10.001.
Hebali, H., Tounsi, A., Houari, M. S. A., Bessaim, A. and Bedia, E. A. A. (2014), "New quasi-3D hyperbolic shear deformation theory for the static and free vibration analysis of functionally graded plates", *J. Eng. Mech.*, **140**(2), 374-383. https://doi.org/10.1061/(ASCE)EM.1943-7889.0000665.
Heyliger, P. R. and Reddy, J. N. (1988), "A higher order beam finite element for bending and vibration problems", *J. Sound Vib.*, **126**(2), 309-326. https://doi.org/10.1016/0022-460X(88)90244-1.
Houari, M.S.A., Tounsi, A., Bessaim, A. and Mahmoud, S.R. (2016), "A new simple three-unknown sinusoidal shear deformation theory for functionally graded plates", *Steel Compos. Struct.*, **22**(2), 257-276. https://doi.org/10.12989/scs.2016.22.2.257.
Lu, Y., Ganesan, Y. and Lou, J. (2010), "A multi-step method for in situ mechanical characterization of 1-D nanostructures using a novel micromechanical device", *Experimental Mech.*, **50**(1), 47-54. https://doi.org/10.1007/s11340-009-9222-0
Kant, T. and Gupta, A. (1988), "A finite element model for a higher-order shear-deformable beam theory", *J. Sound Vib.*, **125**(2), 193-202. https://doi.org/10.1016/0022-460X(88)90278-7.
Karama, M., Afaq, K. S. and Mistou, S. (2003), "Mechanical behaviour of laminated composite beam by the new multi-layered laminated composite structure model with transverse shear stress continuity", *J. Solids Struct.*, **40**(6), 1525-1546. https://doi.org/10.1016/S0020-7683(02)00647-9.
Khdeir, A. A. and Reddy, J. N. (1997), "An exact solution for the bending of thin and thick cross-ply laminated beams", *Compos. Struct.*, **37**(2), 195-203. https://doi.org/10.1016/S0263-8223(97)80012-8.
Levinson, M. (1981), "Further results of a new beam theory", *J. Sound Vib.*, **77**(3), 440-444. https://doi.org/10.1016/S0022-460X(81)80180-0.
Matsunaga, H. (1996), "Buckling instabilities of thick elastic beams subjected to axial stresses", *Comput. Struct.*, **59**(5), 859-868. https://doi.org/10.1016/0045-7949(95)00306-1.
Matsunaga, H. (1996), "Free vibration and stability of thin elastic beams subjected to axial forces", *J. Sound Vib.*, **191**(5), 917-933. https://doi.org/10.1006/jsvi.1996.0163.
Matsunaga, H. (1999), "Vibration and buckling of deep beam-columns on two-parameter elastic foundations", *J. Sound Vib.*, **228**(2), 359-376. https://doi.org/10.1006/jsvi.1999.2415.
Menasria, A., Bouhadra, A., Tounsi, A., Bousahla, A. A. and Mahmoud, S. R. (2017), "A new and simple HSDT for thermal stability analysis of FG sandwich plates", *Steel Compos. Struct.*, **25**(2), 157-175. https://doi.org/ 10.12989/scs.2017.25.2.157.
Meziane, M. A. A., Abdelaziz, H. H. and Tounsi, A. (2014), "An efficient and simple refined theory for buckling and free vibration of exponentially graded sandwich plates under various boundary conditions", *J. Sandwich Struct. Mater.*, **16**(3), 293-318. https://doi.org/10.1177/1099636214526852.
Wang, G. F. and Feng, X. Q. (2009), "Timoshenko beam model for buckling and vibration of nanowires with surface effects", *J. Physics D Appl. Physics*, **42**(15), 155411. https://doi.org/10.1186/1556-276X-7-201.
Miller, R.E. and Shenoy, V.B. (2000), "Size-dependent elastic properties of nanosized structural elements", *Nanotechnology*, **11**(3), 139.
Murty, K. (1984), "Toward a consistent beam theory", *AIAA J.*, **22**(6), 811-816. https://doi.org/10.2514/3.8685.
Nguyen, N.T., Hui, D., Lee, J. and Nguyen-Xuan, H. (2015), "An efficient computational approach for size-dependent analysis of functionally graded nanoplates", *Comput. Methods Appl. Mech. Eng.*, **297**, 191-218. https://doi.org/10.1016/j.cma.2015.07.021.
Nguyen, N.T., Kim, N.I. and Lee, J. (2014), "Analytical solutions for bending of transversely or axially FG nonlocal beams", *Steel Compos. Struct.*, **17**(5), 641-665. https://doi.org/10.12989/scs.2014.17.5.641.
Rao, S. R. and Ganesan, N. (1995), "Dynamic response of tapered composite beams using higher order shear deformation theory", *J. Sound Vib.*, **187**(5), 737-756. https://doi.org/10.1006/jsvi.1995.0560.
Reddy, J. N. (1984), "A simple higher-order theory for laminated composite plates", *J. Appl. Mech.*, **51**(4), 745-752. https://doi.org/10.1115/1.3167719.
Reddy, J. N. (2002), *Energy principles and variational methods in applied mechanics,* John Wiley & Sons., NJ, U.S.A.
Rehfield, L.W. and Murthy, P.L.N. (1982), "Toward a new engineering theory of bending- Fundamentals", *AIAA J.*, **20**(5), 693-699. https://doi.org/10.2514/3.7938.
Saidi, H., Tounsi, A. and Bousahla, A.A. (2016), "A simple hyperbolic shear deformation theory for vibration analysis of thick functionally graded rectangular plates resting on elastic foundations", *Geomech. Eng.*, **11**(2), 289-307. https://doi.org/10.12989/gae.2016.11.2.289.
Sharma, P., Ganti, S. and Bhate, N. (2003), "Effect of surfaces on the size-dependent elastic state of nano-inhomogeneities", *Appl. Phys. Lett.*, **82**(4), 535-537. https://doi.org/10.1063/1.1539929.
Shenoy, V. B. (2002), "Size-dependent rigidities of nanosized torsional elements", *J. Solids Struct.*, **39**(15), 4039-4052. https://doi.org/10.1016/S0020-7683(02)00261-5.
Shenoy, V. B. (2005), "Atomistic calculations of elastic properties of metallic fcc crystal surfaces", *Phys. Rev. B*, **71**(9), 094104. https://doi.org/10.1103/PhysRevB.71.094104.
Soldatos, K. P. (1992), "A transverse shear deformation theory for homogeneous monoclinic plates", *Acta Mechanica*, **94**(3), 195-220. https://doi.org/10.1007/BF01176650.
Stein, M. (1989), "Vibration of beams and plate strips with three-dimensional flexibility", *J. Appl. Mech.*, **56**(1), 228-231. https://doi.org/10.1115/1.3176054.
Subramanian, P. (2006), "Dynamic analysis of laminated composite beams using higher order theories and finite elements", *Compos. Struct.*, **73**(3), 342-353. https://doi.org/10.1016/j.compstruct.2005.02.002.
Sun, C. Q., Tay, B. K., Zeng, X. T., Li, S., Chen, T. P., Zhou, J. I., Bai, H.L. and Jiang, E. Y. (2002), "Bond-order–bond-length–bond-strength (bond-OLS) correlation mechanism for the shape-and-size dependence of a nanosolid", *J. Phys. Condensed Matt.*, **14**(34), 7781. https://doi.org/10.1088/0953-8984/14/34/301.
Tebboune, W., Benrahou, K. H., Houari, M. S. A. and Tounsi, A. (2015), "Thermal buckling analysis of FG plates resting on elastic foundation based on an efficient and simple trigonometric shear deformation theory", *Steel Compos. Struct.*, **18**(2), 443-465. https://doi.org/10.12989/scs.2015.18.2.443.
Thai, H. T. and Vo, T. P. (2012), "Bending and free vibration of functionally graded beams using various higher-order shear

deformation beam theories", *J. Mech. Sci.*, **62**(1), 57-66. https://doi.org/10.1016/j.ijmecsci.2012.05.014.

Thai, S., Thai, H. T., Vo, T. P. and Patel, V. I. (2017), "Size-dependant behaviour of functionally graded microplates based on the modified strain gradient elasticity theory and isogeometric analysis", *Comput. Struct.*, **190**, 219-241. https://doi.org/10.1016/j.compstruc.2017.05.014.

Thai, S., Thai, H. T., Vo, T. P. and Reddy, J. N. (2017), "Post-buckling of functionally graded microplates under mechanical and thermal loads using isogeomertic analysis", *Eng. Struct.*, **150**, 905-917. https://doi.org/10.1016/j.engstruct.2017.07.073.

Timoshenko, S. P. (1921), "LXVI. On the correction for shear of the differential equation for transverse vibrations of prismatic bars", *The London, Edinburgh Dublin Philosophical Mag. J. Sci.*, **41**(245), 744-746. https://doi.org/10.1080/14786442108636264.

Tounsi, A., Houari, M. S. A. and Benyoucef, S. (2013), "A refined trigonometric shear deformation theory for thermoelastic bending of functionally graded sandwich plates", *Aerosp. Sci. Technol.*, **24**(1), 209-220. https://doi.org/10.1016/j.ast.2011.11.009.

Touratier, M. (1991), "An efficient standard plate theory", *J. Eng. Sci.*, **29**(8), 901-916. https://doi.org/10.1016/0020-7225(91)90165-Y.

Trinh, L. C., Nguyen, H. X., Vo, T. P. and Nguyen, T. K. (2016), "Size-dependent behaviour of functionally graded microbeams using various shear deformation theories based on the modified couple stress theory", *Compos. Struct.*, **154**, 556-572. https://doi.org/10.1016/j.compstruct.2016.07.033.

Trinh, L. C., Vo, T. P., Thai, H. T. and Mantari, J. L. (2017), "Size-dependent behaviour of functionally graded sandwich microplates under mechanical and thermal loads", *Compos. Part B Eng.*, **124**, 218-241. https://doi.org/10.1016/j.compositesb.2017.05.042.

Trinh, L. C., Vo, T. P., Thai, H. T. and Nguyen, T. K. (2018), "Size-dependent vibration of bi-directional functionally graded microbeams with arbitrary boundary conditions", *Compos. Part B Eng.*, **134**, 225-245. https://doi.org/10.1016/j.compositesb.2017.09.054.

Vlasov, V.Z. (1966), "Beams, plates and shells on elastic foundations", *Israel Program for Scientific Translations*, Jerusalem.

Wang, B., Zhao, J. and Zhou, S. (2010), "A micro scale Timoshenko beam model based on strain gradient elasticity theory", *European J. Mech. A/Solids*, **29**(4), 591-599. https://doi.org/10.1016/j.euromechsol.2009.12.005.

Wang, G. F. and Feng, X. Q. (2009), "Surface effects on buckling of nanowires under uniaxial compression", *Appl. Phys. Lett.*, **94**(14), 141913. https://doi.org/10.1063/1.3117505.

Yahia, S. A., Atmane, H. A., Houari, M. S. A. and Tounsi, A. (2015), "Wave propagation in functionally graded plates with porosities using various higher-order shear deformation plate theories", *Struct. Eng. Mech.*, **53**(6), 1143-1165. https://doi.org/10.12989/sem.2015.53.6.1143.

Zemri, A., Houari, M. S. A., Bousahla, A. A. and Tounsi, A. (2015), "A mechanical response of functionally graded nanoscale beam: an assessment of a refined nonlocal shear deformation theory beam theory", *Struct. Eng. Mech.*, **54**(4), 693-710. https://doi.org/10.12989/sem.2015.54.4.693